Nanoscale

Accepted Manuscript

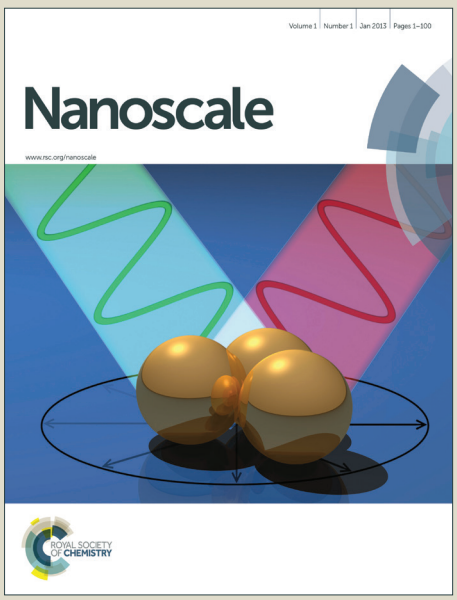

This is an *Accepted Manuscript*, which has been through the Royal Society of Chemistry peer review process and has been accepted for publication.

Accepted Manuscripts are published online shortly after acceptance, before technical editing, formatting and proof reading. Using this free service, authors can make their results available to the community, in citable form, before we publish the edited article. We will replace this *Accepted Manuscript* with the edited and formatted *Advance Article* as soon as it is available.

You can find more information about *Accepted Manuscripts* in the Information for Authors.

Please note that technical editing may introduce minor changes to the text and/or graphics, which may alter content. The journal's standard Terms & Conditions and the Ethical guidelines still apply. In no event shall the Royal Society of Chemistry be held responsible for any errors or omissions in this *Accepted Manuscript* or any consequences arising from the use of any information it contains.

ROYAL SOCIETY OF CHEMISTRY

www.rsc.org/nanoscale

Laser-Ablation Production of Graphene Oxide Nanostructures: from Ribbons to Quantum Dots

T. N. Lin[1], K. H. Chih[2], C. T. Yuan[1], J. L. Shen[1]*, C. A. J. Lin[3], and W. R. Liu[4]

[1]Physics Department, Chung Yuan Christian University, Chung-Li, Taiwan

[2]Master Program in Nanotechnology at CYCU, Chung Yuan Christian University, Chung-Li, Taiwan

[3]Department of Biomedical Engineering, Chung Yuan Christian University, Chung-Li, Taiwan

[4]Department of Chemical Engineering, Chung Yuan Christian University, Chung-Li, 32023, Taiwan

*Correspondence to: jlshen@ cycu.edu.tw

A new one-step method for the preparation of graphene oxide (GO) nanostructures has been developed by pulsed laser ablation in GO solution. The formation of different shapes of GO nanostructures such as ribbons, nanoflakes (including nano-squares, nano-rectangles, nano-triangles, nano-hexagons, and nano-disks) and quantum dots have been demonstrated by scanning electron microscopy and transmission electron microscopy. Photoreduction for the GO occurred during irradiation by the pulsed laser. The GO quantum dots exhibit a blue photoluminescence, originating from recombination of the localized carriers in the zigzag-edge states.

1. INTRODUCTION

Recently, the shape-dependent graphene and/or graphene oxide (GO) nanostructures have attractive much attention, both for fundamental reasons and for their potential applications.[1-5] Graphene nanoflakes and nanoribbons with different shaped edges have been predicted to present different electronic and magnetic properties.[5-6] For instance, graphene nanoribbons with zigzag or armchair shaped edges are both semiconductors with direct band gaps. However, the origins of the band gaps for different types of edge are different. The graphene nanoribbons with zigzag edges come from a staggered sublattice potential due to spin ordered state at the edges, while the ones with armchair edges originate from the quantum confinement associated with edge effects.[7] Among the graphene nanostructures, small fragments of graphene or GO with lateral dimensions less than 100 nm have been termed graphene quantum dots (GQDs).[8-11] Such quantum dots produce discrete band gaps and exhibit fascinating properties, such as low toxicity, biocompatibility, and photoluminescence (PL). GQDs with different shapes and sizes have been reported to exhibit

Nanoscale Accepted Manuscript

anomalous visible PL.[2] The PL behaviors were attributed to the circular-to-polygonal-shape and corresponding edge-state effects of GQDs on the basis of the high-resolution transmission electron microscopy (HRTEM) results.[2] Several reports have indicated that graphene or GO nanostructures with different shapes may open a possible way to a wide variety of applications in electronic and optoelectronic devices.[1-2,6] Therefore, it is essential to develop a vehicle for the preparation of the graphene (or GO) nanosturctures with different shapes to exploit their properties and applications. Shape-dependent graphene nanostructures have been produced by hydrothermal(chemical) cutting of graphene sheets, mechanical cutting of exfoliated graphene, patterning epitaxially grown graphenes, or diamond-edge-induced nanotomy of graphite into graphite nanoblocks, which are then exfoliated.[1-4] However, these methods are sometimes limited by the critical synthesis conditions and time consuming, since some methods need many synthesis steps. It is therefore desirable to develop a one-step, low-cost, and fast method to prepare graphene (or GO) nanostructures with a variety of shapes.

Pulsed laser ablation (PLA) in liquids has been used to produce highly non-equilibrium conditions with local high temperatures and high pressures, leading to complex reactions and the growth of ablated species.[12] This technique is very efficient for generating anomalous phenomena and/or obtaining nanomaterials on a mass scale. Recently, PLA of highly oriented pyrolytic graphite (HOPG) in water have been employed for the synthesis of graphene-related materials.[13-14] The exfoliation of HOPG can be achieved and produces free standing reduced GOs at water-air interface.[14] Porous graphene with a pore dimension of ~20 nm and GQDs with dimensions of about 2-5 nm have also been successfully synthesized using this method.[13] On the other hand, pulsed laser irradiation has been used as an effective route for reduction of GO with a short reaction time.[15-16] The degree of reduction and the hydrophobicity of GO suspension can be finely varied by a pulsed laser irradiation.[17] However, so far, PLA has not been employed to produce GO nanostructures from an aqueous GO solution, which is expected to be a fast and convenient technique. In this study, we develop a strategy for the synthesis of the shape-dependent GO nanostructures using PLA. With a high fluence of laser energy (~ 2.58 J/cm^2), GO sheets can be converted into ribbons, nanoflakes (including nano-squares, nano-rectangles, nano-triangles, nano-hexagons, and nano-disks) and quantum dots by controlling the irradiation time. Structural, physical and chemical properties of the GO nanostructures with different shapes were examined by field emission scanning electron microscopy (FE-SEM), Transmission electron microscopy (TEM), Ultraviolet-visible (UV-Vis) absorption spectra, X-ray photoelectron spectra (XPS), Raman spectroscopy, and PL measurements. The PL mechanism of graphene oxide quantum dots (GOQDs) were also investigated.

2. EXPERIMENTAL SECTION

The GO aqueous solution (275 mg/L) for fabrication of the GO nanostructures was purchased from *Graphene Supermarket* (U.S.A.) and used without further purifications. The

Nanoscale Accepted Manuscript

thickness and size of the GO flakes were one atomic layer (at least 80-%) and 0.5-5μm, respectively.[18] The GO solution was placed in a quartz cell on a rotational stage with an angular velocity of 80 rpm and exposed to the pulses from the OPO pulsed laser (415 nm, 10 Hz, 10 ns) (Fig. 1(a)). The PLA of GO were carried out under the fluence of 2.58 J/cm^2 with duration times from 5 to 40 min. For comparison, we also performed the PLA of GO with lower fluences (from 0.26 to 2.1 J/cm^2). The suspension product was filtered before characterization using syringe filters (Millipore, 0.22μm pore size).

A field emission scanning electron microscopy (FE-SEM) (Hitachi S-4100) and a high resolution transmission electron microscopy (HRTEM) (JEOL JEM-2100F) were used to analyze the morphology and structures. Ultraviolet-visible (UV-Vis) measurements were carried out with the spectrophotometer (Varian Cary 50 UV) over a spectral range of 200-600 nm. The Raman spectra were carried out by a micro Raman spectroscopy system with laser frequency of 532 nm as the excitation source. The composition of the products was evaluated by X-ray photoelectron spectra (Thermo Scientific K-Alpha ESCA instrument) equipped with a monochromatized Al-Kα X-ray source at 1486.6 eV. The excitation-dependent PL spectra were analyzed using the spectrofluorometer (Horiba Jobin Yvon FluoroMax-4). A pulsed laser with a wavelength of 260 nm, a repetition frequency of 20 MHz, and a duration of 250 fs was used as the excitation source for time-resolved PL studies. The collected luminescence was dispersed by a 0.75 m spectrometer and detected with the photomultiplier tube. Time-resolved PL were performed using the technique of time-correlated single-photon counting (TCSPC). The steady-state and time-resolved PL was measured at room temperature.

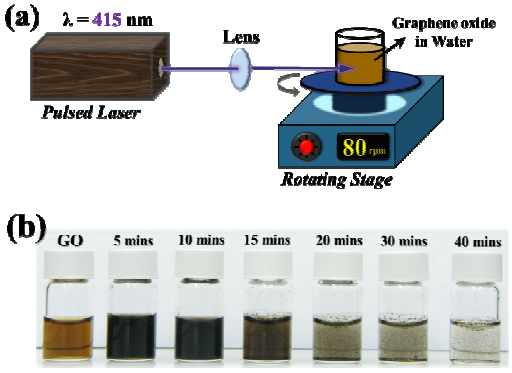

Fig. 1. (a) Schematic representation of the experimental setup (b) Photographs of the GO solution before and after irradiation by a pulsed laser.

3. RESULTS AND DISCUSSION

Upon laser irradiation, the color of the GO suspension changed with time. The light brown color of the original GO solution changed to black as the irradiation time increased from 0-10 min (Fig. 1(b)) This kind of color change is attributed to the partial restoration of an sp^{2}π-conjugated network within the carbon structure and can be considered as a sign of

Nanoscale Accepted Manuscript

reduction of the GO nanosheets.[19] For an irradiation time greater than 10 min, the suspension started to precipitate and some black aggregates on the top and bottom surfaces of the liquid. This phenomenon could be interpreted by the formation of web-like carbon aggregates or black coagulations.[20] It is noteworthy that no precipitation or bleaching in the GO suspension was observed for a lower fluence of laser energy (e.g. ~ 0.1 J/cm^2). At low fluences of laser, the color of the GO solution changed to black and remained so after an irradiation time of 30 min.

Fig. 2 shows the optical UV-Vis absorption spectra of GO suspension for laser exposures from 0 to 40 min. It can be seen that the optical absorption of the untreated GO was dominated by a peak at 230 nm, which is typically assigned as the π-π* transitions of aromatic sp^2 domains.[16] A shoulder around 300 nm is often attributed to n-π* transitions of the C=O bond in sp^3 hybrid regions.[16] Upon laser irradiation for 0-10 min, the absorption intensity in the whole spectrum increased and the 230-nm peak shifted toward the long-wavelength region. This red shift is usually observed when GO is reduced, arising from the restoration of the sp^2-bonded carbon C=C and reflecting the increased π electron concentration.[16-17] Thus, we suggest that the red shift of the 230-nm peak is related to the reduction effect of GO under PLA. A similar trend was also observed for the reduction of GO sheets by a progressive pulsed laser irradiation.[17] For laser irradiation more than 10 min, the intensity of the whole spectra decreases pronouncedly. One possible origin of the decreased absorption is owing to precipitation on the surface of the liquid. In addition, the reduction of GO can remove the oxygen-related functional groups from the sp^3 C-O matrix, leading to a decrease of the non-emitting background absorption.[11] The removal of the oxygen-related functional groups will be demonstrated in the XPS analysis later. A new shoulder around 340 nm appeared after irradiation more than 20 min, as likewise reported for some GQD in the UV-Vis absorption spectra.[21]

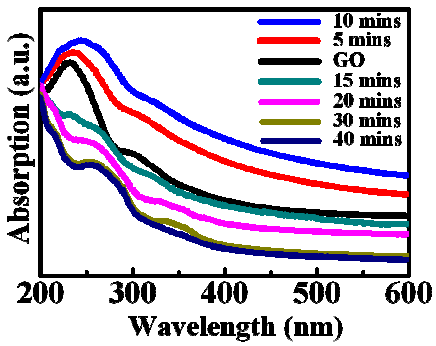

Fig. 2 UV-Vis absorption spectra of the GO solution at different laser irradiation times.

Fig. 3 and Fig. 4 show the SEM images of the as-prepared GO nanostructures before and after PLA. It is obvious that the GO sample possesses a sheet-like morphology before PLA

Nanoscale Accepted Manuscript

(Fig. 3(a)). The size of the GO flakes decreased basically as the irradiation time increased. The propeller-like and tortuous GO ribbons were observed after an irradiation time of ~7 min, as shown in Figs. 3(b) and 3(c), respectively. Figs. 4(a)-(e) indicate the shapes of GO nanoflakes, a few tenths of or hundreds of nanometers in size, for the irradiation time between 10 and 15 min. The produced GO nanoflakes include nano-squares, nano-rectangles, nano-hexagons, nano-triangles, and nano-disks. The corresponding shape distribution of these GO nanostructures is displayed in Fig. 4(f) by randomly counting more than 150 nanoflakes.

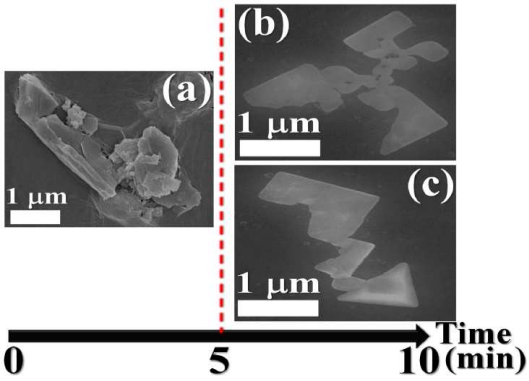

Fig. 3 SEM images of the GO after irradiation times from (a) 0 min to (b-c) 7 min.

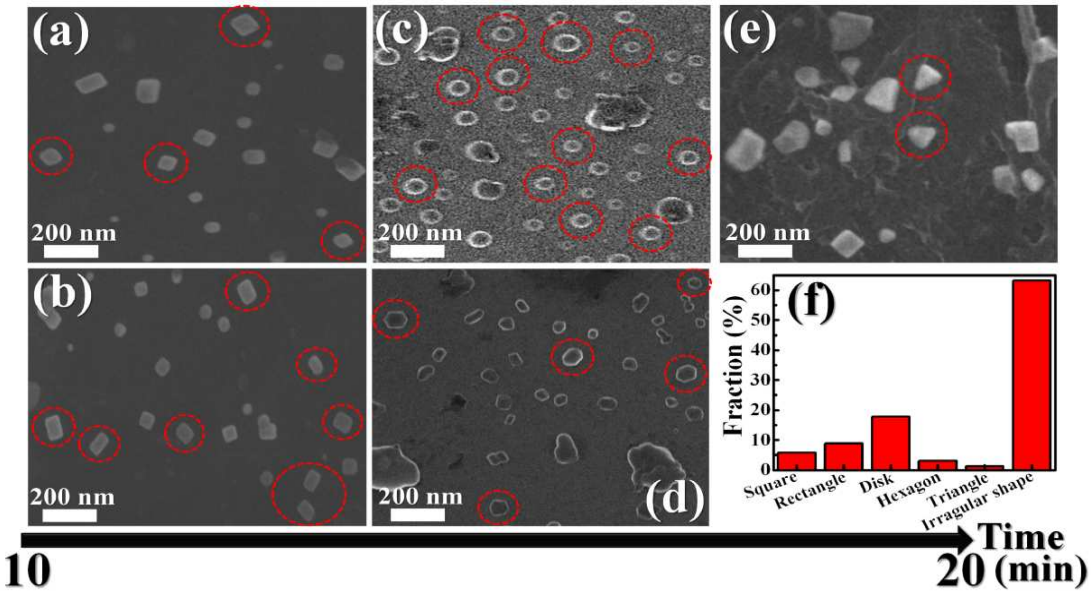

Fig. 4 SEM images of the GO nanoflakes with different shapes (marked by dashed circles): (a) squares, (b) rectangles, (c) disks, (d) hexagons, and (e) triangles. The yield of each kind of nanoflakes is shown in (f).

In graphene, different geometrical terminations of two-dimensional lattice lead to 0D graphene nanoflakes. Graphene nanoflakes include a large number of dangling bonds of edge atoms. Therefore, they are unstable and have large configurational degrees of freedom, leading to a variety of different shapes such as squares, rectangles, hexagons, triangles, rhombs, and disks.[5-6] It has been reported that the structure stability of graphene nanoflakes

Nanoscale Accepted Manuscript

depends on the size, shape, temperature, charge, defects, and interaction with other chemical groups.[22] For example, the hexagonal nanoflakes with armchair edges are most likely to be produced, provided that sufficient hydrogen is present during synthesis to facilitate dihydride edge and corner pasivation.[23] Also, shapes of graphene nanoflakes may change from triangle to hexagon when the ambient temperature is increased.[24] In our case, we have produced nano-squares, nano-rectangles, nano-hexagons, nano-triangles, and nano-disks using PLA with the irradiation time between 10 and 15 min. Although the graphene nanostructures with different shapes have been prepared by other methods before.[1-4] With appropriate fluences of the laser energy as well as the irradiation time, we can prepare these GO nanoflakes in a one-step process. For applications, it is desirable to control and/or separate the different shapes of GO nanoflakes. For the separation of nanoflakes by size, it can be achieved using controlled centrifugation.[25] However, the controlled technique of specific shapes in nanoflakes is still challenging to experimentalists.[22] This issue needs further investigation since that will be important in the development of graphene-based nanotechnology.

After the irradiation time more than ~20 min, smaller GO nanostructures could be produced and their sizes are beyond the resolution capability of SEM. To further elucidate the structure, TEM imaging analysis was performed. Fig. 5(a) displays the TEM images of the GO products fabricated by PLA for 30 min. It was found that the GO nanostructures decreased further in size, becoming GOQDs. The high resolution TEM (HRTEM) of a GOQD exhibits an crystalline structure with an interplanar spacing of 0.214 nm, corresponding to the (102) lattice fringes of graphene (Fig. 5(b)).[26-27] Statistical analyses of the TEM images gave a Gaussian distribution as shown in Fig. 5(c). The sizes of these GOQDs were mainly distributed in the range of 5-40 nm, with an average of 14 nm and a full width at half maximum (FWHM) of 2 nm.

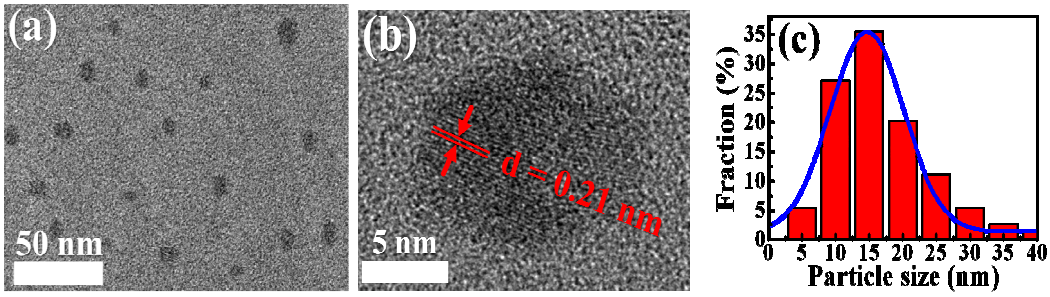

Fig. 5 (a) A TEM image of GOQDs fabricated by PLA for 30 min. (b) high-resolution TEM image of an individual GOQD. (c) size distribution of GOQDs. The solid line indicates the Gaussian fit.

Fig. 6 shows the SEM images of GO products after PLA of 15 min with different irradiation energies. Irregular GO sheets with the average sizes with a dimension of ~1 μm were found for the laser energy of 0.26 J/cm^2 (Fig 6(a)). After laser ablation with energy of 1.45 J/cm^2 (Fig 6(b)), GO pieces become smaller with a size of ~0.2-0.5 μm. When the laser energy is increased up to 2.09 J/cm^2, small GO pieces varied from ~0.1 to ~0.3 μm were

Nanoscale Accepted Manuscript

produced, as indicated in Fig 6(c). These results suggest that the size of GO nanostructures can be tuned over a range by varying the laser pulse energy. However, no acute edges of GO nanostructures were observed when the PLA was carried out with low energies.

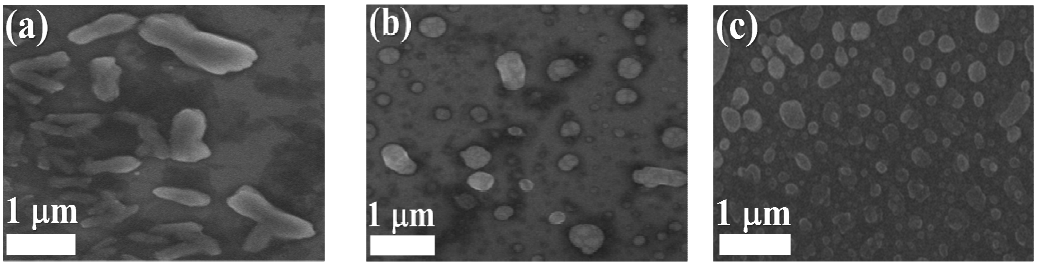

Fig. 6 SEM images of the GO nanosheets after different irradiation energy: (a) 0.26 J/cm^2 , (b) 1.45 J/cm^2, and (c) 2.09 J/cm^2.

Raman spectroscopy is a useful technique for examining the ordered/disordered crystal structures of graphene-based materials. Fig. 7(a) shows the Raman spectra before and after the PLA of GO, revealing typical bands of GO structures: the D band at ~1351 cm^{-1} and G band at ~1591 cm^{-1}. The D and G bands represent the defect-induced breathing mode of aromatic rings and the optical E_{2g} phonons at the Brillouin zone center, respectively.[1] In addition to the D and G bands, 2D band at ~2590 cm^{-1}, D+G band at ~ 2917 cm^{-1} and 2G band at ~3120 cm^{-1} can be seen in Fig. 6(b). The 2D band is the second order of the D band, which can be associated with the stacking order in GO lattice.[30] The peak of the 2D band is shifted to higher frequencies and its intensity is decreased as the irradiation time of PLA increases. The blue shift of 2D band in GO is a fingerprint of reduction in GO owing to stronger coupling accompanied by removal of trapped interlayer species and functional groups.[3] This result is in good agreement with that of UV-Vis absorption in Fig. 2.

It is well documented that the intensity ratio of the D and G bands is a measure of the size of the sp^2 regions in a network of sp^3- and sp^2- bonded carbon.[28] The average crystallite size of sp^2 domain L_a can be determined according to the modified Tuinstra-Koenig relation:[29]

$$L_a(nm) = (2.4\times10^{-10})\lambda^4(\frac{I_D}{I_G})^{-1}, \quad (1)$$

where λ is the excitation wavelength, I_D is the integrated intensity of the D band, and I_G is the integrated intensity of the G band. The open squares in Fig. 7(c) show the corresponding changes in L_a with respect to the laser irradiation time, with L_a increasing by about two times with the increase of the irradiation time. The increase of L_a is associated with the formation of new sp^2 carbon atoms in the GO lattice after PLA.

Nanoscale Accepted Manuscript

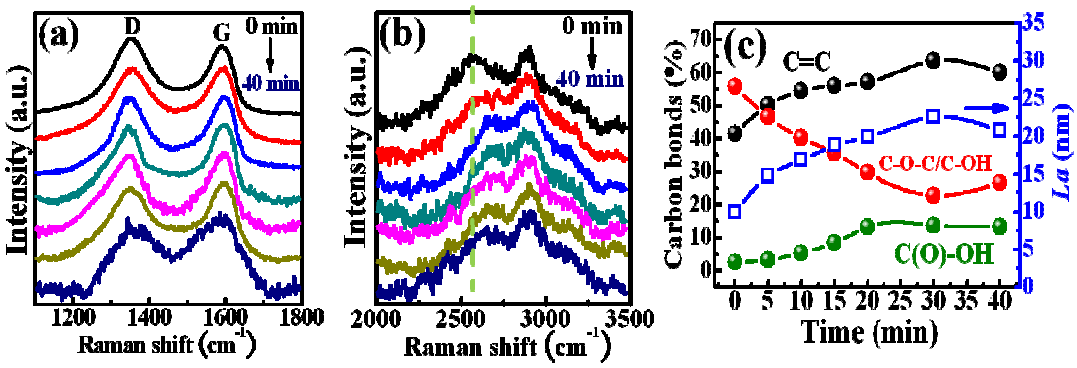

Fig. 7 (a-b) Raman scattering spectra of GO nanostructures at different laser irradiation times (c) the average size of the sp^2 domain obtained from Raman scattering as a function of the laser irradiation time. Relative concentrations of different carbon bonds in GO nanostructues identified by XPS as a function of the irradiation time are also shown. The lines are guides for the eyes.

To investigate the changes in chemical structure of all samples, XPS measurements were carried out. The XPS spectra in Fig. 8 display the C1s carbon of GO samples before and after PLA. Deconvolution of the C1s peak suggested the presence of three bands at 284.4, 286.3, and 288.4 eV binding energies, which corresponded to the sp^2 aromatic carbon (C=C), hydroxyl(C-OH)/epoxy groups(C-O-C), and carboxyl groups (C(O)-OH), respectively.[31-32] Considerable contributions of the oxygen-containing functional groups were observed for the sample before irradiation (Fig. 8(a)), indicating that untreated GO is very rich in oxygen. After PLA, the percentage at the 286.3-eV binding energy decreases from 56 to 25 % as the irradiation time increased from 0 to 30 min. This demonstrated that hydroxyl/epoxy groups decreased significantly on GO sheets with the increase of PLA. Meanwhile, the percentage at the 284.4-eV binding energy increased with the irradiation time, indicating an increase of sp^2 aromatic carbon after PLA. The decrease of hydroxyl/epoxy groups and the increase of sp^2 aromatic carbon are matched with the previous report in the reduction of GO by laser irradiation.[17] We thus confirm the reduction of GO nanosheets upon increasing the irradiation time. For the binding energy at 288.4-eV, the percentage increased as the irradiation time increased, revealing that more carboxyl groups were generated during PLA. Fig. 7(c) displays the evolution of the C1s carbon bonds in GO extracted from XPS as a function of the irradiation time, indicating that the trend of the increased sp^2 domains agrees with that of the Raman results. Also, compared with the evolution of the 284.4- and 286.3-eV binding energies, we deduced that the increased contribution of the sp^2 aromatic carbon mainly resulted from the decreased amount of hydroxyl/epoxy groups, as shown in Fig. 7(c).

Nanoscale Accepted Manuscript

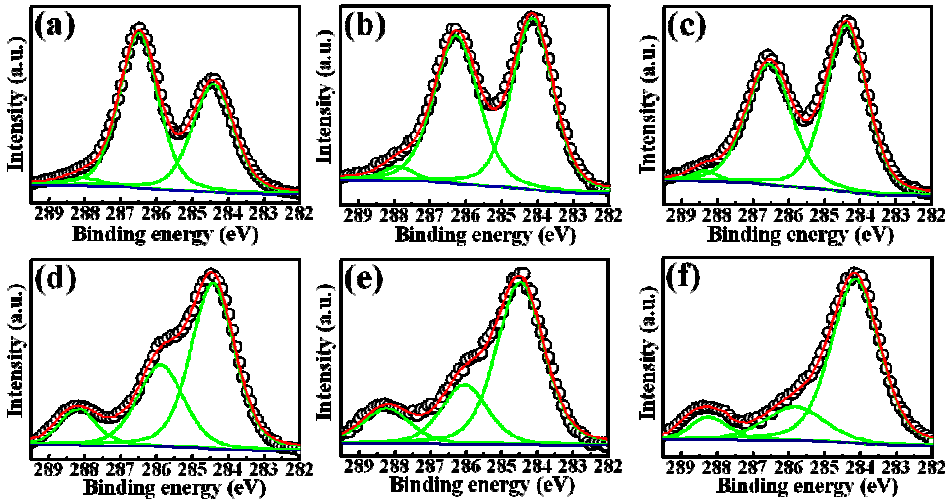

Fig. 8 XPS spectra of C 1s of GO nanostructures after different irradiation time: (a) 0 min, (b) 5 min, (c) 10 min, (d) 15 min, (e) 20 min, and (f) 30 min.

According to the above characterizations, we have suggested a possible mechanism for the reduction and ablation of GO by a pulsed laser. At the start, the mechanism of the reduction in GO is attributed to the photochemical desorption of oxygen groups.[34] During laser irradiation, the energy from the recombination of photoexcited carriers can be converted for water dissociation into molecular oxygen and hydrogen.[13] Molecular hydrogen are inherently reducing agents, giving rise to the removal of oxygen-containing functional groups from the GO lattice. The reduction of GO was confirmed by the result of the XPS (Fig. 8), which shows the decreased hydroxyl/epoxy groups and the increased sp^2 aromatic carbon during PLA. With the progression of the laser irradiation, the energy absorbed by the GO increases, giving rise to local high temperatures and high pressures. Accordingly, high strain rates are generated in the surrounding liquid upon implosion, which can fragment the GO into smaller pieces and reestablishes the lattice defects.[32] Thus, the carbon bonds and/or carbon backbone are broken, resulting in significant morphological changes in GO and producing the GO nanostructures with a variety of shapes.

Fig. 9(a) shows the PL of the GOQDs with different excitation wavelength. When the excitation wavelength is changed from 320 to 400 nm, the PL peak shifts monotonically from 455 to 510 nm and its intensity changes rapidly. The PL emission on excitation wavelength is similar to that of GOQDs reported previously.[10,34] The excitation-dependent PL has been attributed to different emitting species or the localization of electron-hole pairs owing to the isolated sp^2 clusters within the sp^3 matrix.[20] In Fig. 9(a), the PL spectra show a PL peak at 460 nm when excited with the wavelength at 340 nm, which approximates that of the GOQDs synthesized by a chemical acid treatment method.[34] Thus, the above results demonstrate that the PL properties of our GOQDs are in agreement with those of the reported one. The PL

Nanoscale Accepted Manuscript

quantum yield of GOQDs was measured to be 1.8%, which is lower respect to that reported in GQDs (7-11%) but no result reported in literature for GOQDs.[35-36] The low PL quantum yield may be related to the highly defective structures on the surfaces of GOQDs. It is expected that when the surface is modified by functional groups or/and the sites of nonradiative recombination are passivated, the PL quantum yield can be greatly improved.

Fig. 9(b) displays the PL of the GOQDs generated by the different irradiation time when an excitation wavelength of 260 nm is used. The PL intensity of the investigated GOQDs as a function of the irradiation time is shown in Fig. 9(c). The PL intensity reached a maximum at the irradiation time of 30 min and then decreases with further irradiation. It has been reported that the PL intensity in GQDs is dependent on the chemical nature of their surfaces.[37] The hybridization of the carbon backbone and the carboxyl groups at the edge has been demonstrated to be associated with the green luminescence. On the other hand, the epoxy and hydroxyl groups are nonradiative recombination centers of electron-hole pairs, which result in a decrease of luminescence in GO.[38] Based on the XPS results, we deduce that the increase of PL can be correlated with the decreased epoxy/hydroxyl groups and the increased carboxyl groups during PLA.

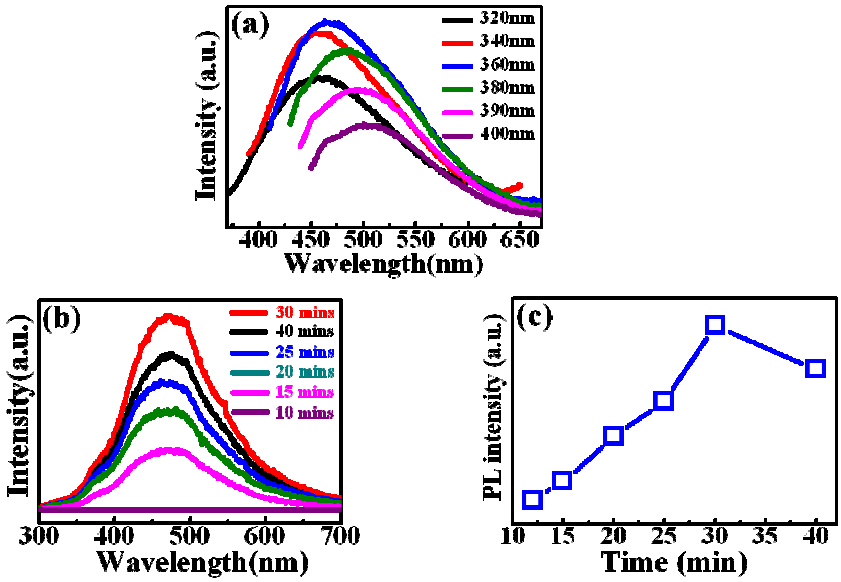

Fig. 9 (a) PL spectra of GOQDs with varying excitation wavelengths. (b) PL spectra of GOQDs prepared by pulsed laser ablation with different irradiation times (c) PL intensity as a function of the irradiation time of the GOQDs (the line is a guide to the eyes);

Time-resolved PL decay measurements can provide a complementary technique to study the PL mechanism of GOQDs, using the kinetics of electron-hole recombination as a probe. The open squares in Fig. 10(a) display the PL decay profile of the GOQD sample under excitation of the 260 nm laser with PLA for 30 min. The PL profile can be well fitted by a biexponential function:

Nanoscale Accepted Manuscript

$$I(t) = A_f e^{-\frac{t}{\tau_f}} + A_s e^{-\frac{t}{\tau_s}}, \quad (2)$$

where τ_f (τ_s) represents the decay time of fast (slow) decay, A_f (A_s) represents the amplitude of the fast-decay (slow-decay) component at t = 0. The decay curve in Fig. 10(a) gives time constants of τ_f = 1.53 ns and τ_s = 8.89 ns for the fast and slow decay, respectively. To investigate the PL properties, PL decay profiles with different emission energy were analyzed. The open circles and squares in Fig. 10(b) show the emission energy dependence of the decay time constants. It is found the decay time constants decrease with increasing emission energy, which is a characteristic of the carrier localization.[39] In the carrier localization model, carriers may transfer from a higher energy states into a region of lower energy states before recombination. Thus, two competing processes exist for a given carrier, i.e., transfer to another localized tail states with a lower energy and radiative recombination. The combination of transfer and recombination has been modeled by assuming the density of localized tail states is proportional to $\exp(-E/E_0)$, where E_0 describes the depth of the localized states. The observed lifetime $\tau(E)$ can be expressed by the following equation:[39]

$$\tau(E) = \frac{\tau_r}{1+\exp[(E-E_{me})/E_0]}, \quad (3)$$

where τ_r is the radiative lifetime and E_{me} is defined by a definite energy for which the decay time equals the transfer time. The fitted PL decay times are plotted with the solid lines in Fig. 10(b). Good fits to the experiment data confirm the existence of carrier localization. In the fits, τ_r, E_{me}, and E_0 were estimated to be 0.72 (3.85) s, 3.02 (2.95) eV, and 82 (135) meV for the fast-(slow-) decay component of PL decay times, respectively.

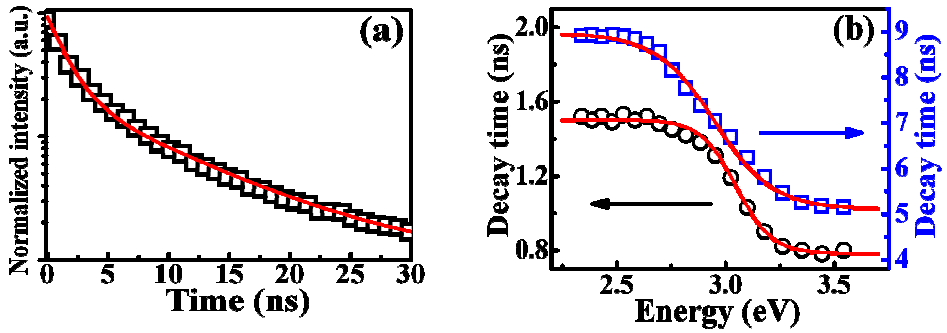

Fig. 10 (a) The PL decay profile of GOQDs monitored at the emission peak (open squares). The solid line is a fit according to Eq. (2). (b) The emission energy dependence of the fast (open circles) and slow(open squares) components for PL decay times. The solid line are fits to Eq. (3) from the carrier localization model.

Graphene is a two dimensional monolayer of carbon atoms packed into a honeycomb

Nanoscale Accepted Manuscript

lattice. In graphene nanostructures the π-network still consists of sp^2- hybridized carbons, but the carbon atoms at the edges are not saturated. Depending on the termination style, the edge geometry of graphene nanostructures can be divided into two kinds: armchair and zigzag. The electronic properties of the armchair and zigzag edges are very different, particularly in the formation of localized states. It has been demonstrated that electronic transport in zigzag graphene nanoribbons takes place via localized states since electrons in zigzag edges are exponentially localized near the Fermi level.[40] On the other hand, no such localized states have been found on in armchair edges of nanorobbins and their electrons are delocalized.[28] According to this argument, we suggest that the PL decay transients in Eq.(2) are related to the decay of carriers in the zigzag edges since it exhibits the behavior of carrier localization (Fig. 10(b)). Hence, the blue PL in GOQDs originates from the recombination of the localized carriers from the zigzag-edge states of GOQDs.

4. CONCLUSION

A one-step method with PLA has developed to prepare GO nanostructures with a variety of shapes. On the basis of SEM and TEM studies, various GO nanostructures such as ribbons, nanoflakes (including nano-squares, nano-rectangles, nano-triangles, nano-hexagons, and nano-disks) and GOQDs have been produced. UV-Vis absorption spectroscopy, Raman spectroscopy and XPS were used to examine the products of GO after PLA, indicating that the PLA leads to photoreduction of the GO nanosheets. The as-prepared GOQDs exhibits a blue PL behavior, making them a good candidate for potential applications in optoelectronics and biomedicine. The PL intensity of the GOQDs was found to vary with the irradiation time, which can be correlated with the concentrations of the oxygen-containing functional groups. The recombination dynamics of GOQDs was also investigated using time-resolved PL. We suggest that the blue PL from GOQDs is associated with recombination of the localized carriers in the zigzag-edge states.

Acknowledgments. This project was supported by the Ministry of Science and Technology in Taiwan under the grant numbers MOST 103-2112-M-033-004-MY3 and NSC 102-2632-M-033-001-MY3

References:

1. N. Mohanty, D. Moore, Z. Xu, T. S. Sreeprasad, A. A. Rodriguez, and V. Berry, *Nature Comm.* 2012, 3, 1834
2. S. Kim, S. W. Hwang, M. Kim, D. Y. Shin, D. H. Shin, C. O. Kim, S. B. Yang, J. H. Park, E. Hwang, S. Choi, G. Ko, S. Sim, C. Sone, H. J. Choi, S. Bae, and B. H. Hong, *ACS Nano* 2012, 6,

Nanoscale Accepted Manuscript

8203.

3. K. S. Novoselov, A. K. Geim, S. V. Morozov, D. Jiang, M. I. Katsnelson, I. V. Grigorieva, S. V. Dubonos, and A. A. Firsov, *Nature*, 2005, 438, 197.
4. C. Berger, Z. Song, X. Li, X. Wu, N. Brown, C. Naud, D. Mayou, T. Li, J. Hass, A. N. Marchenkov, E. H. Conrad, P. First, and W. A. de Heer, *Science*, 2006, 312, 1191.
5. H. Shi, A. S. Barnard, and I. K. Snook, *Nanoscale*, 2012, 4, 6761.
6. S. Dutta and S. K. Pati, *J. Mater. Chem.,* 2010, 20, 8207.
7. Y. Son, M. L. Cohen, and S. G. Louie, *Phys. Rev. Lett.* 2006, 97, 216803.
8. V. Štengl, S. Bakardjieva, J. Henych, K. Lang, and M. Kormunda, *Carbon*, 2013, 63, 537.
9. X. Zhou, Y. Zhang, C. Wang, X. C. Wu, Y. Q. Yang, B. Zheng, H. Wu, S. Guo, and J. Zhang, *ACS Nano*, 2012, 6, 6592-9.
10. F. Liu, M. H. Jang, H. D. Ha, J. H. Kim, Y. H. Cho, and T. S. Seo, *Adv. Mater.*, 2013, 25, 3657.
11. Y. Dong, J. Shao, C. Chen, H. Li, R. Wang, Y. Chi, X. Lin, and G. Chen, *Carbon,* 2012, 50, 4738.
12. G. Yang, *Prog. Mater. Sci*., 2007, 52, 648.
13. P. Russo, A. Hu, G. Compagnini, W. W. Duley, and N. Y. Zhou, *Nanoscale*, 2014, 6, 2381.
14. G. Compagnini, P. Russo, F. Tomarchio, O. Puglisi, L. D'Urso, and S. Scalese, *Nanotechnology*, 2012, 23, 505601.
15. Y. L. Zhang, L. Guo, H. Xia, Q. D. Chen, J. Feng, and H. B. Sun, *Adv. Opt. Mater.*, 2014, 2, 10.
16. V. Abdelsayed, S. Moussa, H. M. Hassan, H. S. Aluri, M. M. Collinson, and M. S. El-Shall, *J. Phys. Chem. Lett*., 2010, 1, 2804
17. S. F. Spanò, G. Isgrò, P. Russo, M. E. Fragalà, and G. Compagnini, *Appl. Phys. A*, 2014, 117 19.
18. Company data. Retrieved from https://graphene-supermarket.com/Dispersion-in-Water-Single-Layer-Graphene-Oxide-175-ml.html.
19. H. A. Becerril, J. Mao, Z. Liu, R. M. Stoltenberg, Z. Bao, and Y. Chen., *ACS Nano*, 2008,2, 463.
20. S. K. Yang, H. B. Zeng, H. P. Zhao, H. W. Zhang, and W. P. Cai, *J. Mater. Chem.*, 2011, 21, 4432.
21. D. Pan, J. Zhang, Z. Li, and M. Wu, *Adv. Mater.*, 2010, 22, 734.
22. H. Shi, A. S. Barnard, and I. K. Snook, *Nanotechnology*, 2012, 23, 065707.
23. A. S. Barnard, and I. K. Snook, *Modelling Simul. Mater. Sci. Eng.*, 2011, 19, 054001.
24. H. Shi, L. Lai, I. K. Snook, and A. S. Barnard, *J. Phys. Chem. C*, 2013, 117, 15375.
25. U. Khan, A. O'Neill, H. Porwal, P. May, K. Nawaz, and J. N. Coleman, *Carbon,* 2012, 50, 470.
26. H. Sun, N, Gao, L. Wu, J. Ren, W. Wei, and X. Qu, *Chem. Eur. J.,* 2013, 19,13362.
27. H. Sun, L. Wu, N. Gao, J. Ren, X. Qu, *ACS Appl. Mater. Interfaces,* 2013, 5, 1174.
28. J. R. Rani, J. Lim, J. Oh, J. W. Kim, H. S. Shin, J. H. Kim, S. Lee, and S. C. Jun, *J. Phys. Chem. C,* 2012, 116, 19010.
29. L. G. Cançado, K. Takai, T. Enoki, M. Endo, Y. A. Kim, H. Mizusaki, A. Jorio, L. N. Coelho, R. Magalhães-Paniago, and M. A. Pimenta, *Appl. Phys. Lett.* 2006*,* 88, 163106.

Nanoscale Accepted Manuscript

30. K. Krihnamoorthy, M. Veerapandian, K. Yun, and S. J. Kim, *Carbon,* 2013, 53, 38.

31. H. W. Tien, Y. L. Huang, S. Y. Yang, J. Y. Wang, and C. C. M. Ma, *Carbon*, 2011, 49, 1550.

32. D. Tan, Y. Yamada, S. Zhou, Y. Shimotsuma, K. Miura, and J. Qiu, *Nanoscale*, 2013, 5, 12092

33. L. Guo, R. Q. Shao, Y. L. Zhang, H. B. Jiang, X. B. Li, S. Y. Xie, B. B. Xu, Q. D. Chen, J. F. Song , and H. B. Sun, *J. Phys. Chem. C*, 2012, 116, 3594.

34. Y. Zhang, H. Gao, J. Niu, and B. Liu, *New J. Chem.*, 2014, 38, 4970.

35. D. Pan, J. Zhang, Z. Li, and M. Wu, *Adv. Mater.*, 2010, 22, 734.

36. L. Minati, S. Torrengo, D. Maniglio, C. Migliaresi, and G. Speranza, *Mater. Chem.Phys.*, 2012, 137, 12.

37. L. Fan, Y. Hu, X. Wang, L. Zhang, F. Li, D. Han, Z. Li, Q. Zhang, Z. Wang, and L. Niu, *Talanta*, 2012, 101, 192.

38. L. Wang, S. J. Zhu, H.Y. Wang, S. N. Qu, Y. L. Zhang, J. H. Zhang, Q. D. Chen, H. L. Xu, W. Han, B. Yang, and H. B. Sun, *ACS Nano,* 2014, 8, 2541.

39. T. Bartel, M. Dworzak, M. Strassburg, A. Hoffmann, A. Strittmatter, and D. Bimberg, *Appl. Phys. Lett.*, 2004, 85, 1946.

40. I. Kleftogiannis, I. Amanatidis, and V. A. Gopar, *Phys. Rev. B*, 2013, 88, 205414.

Nanoscale Accepted Manuscript